

Control Strategies for Dynamic Voltage Support During Faults Using PV Smart Inverter

Rafaella A. F. Santos*. R. Reginatto**

*Western Paraná State University, Foz do Iguaçu, PR,
(e-mail: rafaella.santos4@unioeste.com).

**Center for Engineering and Exact Sciences, Western Paraná State University, Foz do Iguaçu, PR,
(e-mail: romeu@unioeste.br)

Abstract: In recent years, the number and capacity of solar photovoltaic (PV) installations connected to the power system are growing at a rapid pace worldwide. Therefore, power quality issues related to voltage regulation and grid stability are becoming relevant problems for distribution networks and PV owners. To mitigate these impacts, interconnection standards have been amended to add smart features to solar PV inverters as “Smart Inverters”, such as Low Voltage Ride-Through (LVRT) and dynamic voltage support. This paper explores the Volt-VAr control as a dynamic voltage support during faults in smart inverters with LVRT capacity. Furthermore, this work also develops different strategies to deal with DC link voltage level and converter capacity limitation. The simulation results show the reactive power injected to the system, the behavior of the inverter terminal voltage, and the DC link voltage level for different current priority techniques.

Keywords: Photovoltaic (PV); Smart Inverters; Dynamic Voltage Support; LVRT; Volt-VAr; DC link Voltage; Fault.

1. INTRODUCTION

The interconnection of Distributed Generation (DG) based on renewable energy sources to the grid, especially solar photovoltaic (PV), has experienced rapid growth in recent years worldwide (Zhao et al., 2018). In 2019, Brazil surpassed the 1GW mark in DG and the most used source is the PV, with 82,6 thousand micro and mini plants and approximately 870 megawatts (MW) of installed power (ANEEL, 2019).

Nonetheless, the large amount of PV in the power system also makes the distribution network more vulnerable due to its intermittent power output (Lulbadda & Hemapala, 2019). Thus, interconnection standards from different nations across the world have been amended to add smart features to solar PV inverters in view of the increasing threat to the voltage stability of the power system network (Naidu et al., 2019).

IEEE introduced a series of standards called “IEEE 1547 Standard for Interconnection and Interoperability of Distributed Energy Resources with Associated Electric Power System Interface”. Today, this standard is one of the most influential standard for interconnection of all forms of DG, and includes smart features to solar PV inverters (Arbab-Zavar et al., 2019; Lulbadda & Hemapala, 2019; Teodorescu et al., 2011).

The revised IEEE 1547-2018 Standard allows PV inverters to actively regulate the voltage at the Point of Common Coupling (PCC) by compensating reactive power through

Volt-VAr control. Furthermore, the Low Voltage Ride-Through (LVRT) capacity is mandatory, requiring PV inverter to remain connected during voltage sags (Almeida et al., 2020; Jafari et al., 2019; Kashani et al., 2019).

With these new features, the traditional inverter is upgraded to “Smart Inverter,” which has adjustable thresholds and provides decentralized control and greater autonomy to the system. Thus, smart inverters do not disconnect immediately during a disturbance like traditional converters. They shall stay connected to the grid for a specific duration, being able to provide dynamic voltage support, and then trip after the must trip time (Arbab-Zavar et al., 2019; Lulbadda & Hemapala, 2019).

The works of Bravo (2015), Naidu et al. (2019) and Shuvra & Chowdhury (2015) address the controls for dynamic voltage support that provide smart inverters the ability to support network voltage during faults. As an example, Bravo (2015) presents the importance of reactive power control to support network stability and even avoid voltage collapses.

Easley et al., (2020) propose decoupled active and reactive power controls during fault with Low Voltage Ride Through capacity. Thus, the smart inverter adjusts the operating points of the active and reactive power controls according to the grid voltage. The author also presents three strategies for the operation of the photovoltaic system during faults.

The purpose of the present work is to explore the Volt-VAr control for dynamic voltage support during faults in smart

inverters with LVRT capacity. Different strategies to deal with DC link voltage level and converter capacity limitation are developed and their performance analyzed.

This paper is divided into 4 sections. Section 2 deals with the modeling of PV systems. Section 3 introduces the new Smart Inverters features and presents the LVRT and dynamic voltage support modeling. The simulation results are presented in Section 4. Finally, the conclusion will be presented in Section 5, including the analyzes and performance comparisons of the observed variables.

2. PHOTOVOLTAIC SYSTEM MODEL

Grid-connected photovoltaic systems can be classified as either one-stage or two-stage conversion systems, based on the power conversion steps considered. Fig. 1 shows a two-stage conversion system used in this work, which includes a DC-DC converter and a DC-AC converter (inverter).

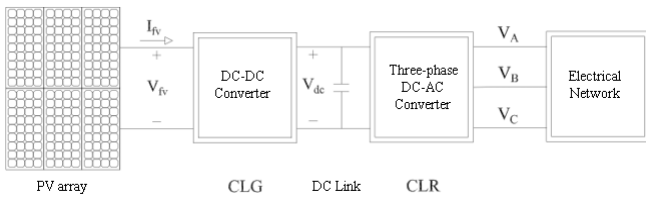


Fig. 1 Two-stage PV system.

In this work, converters are represented in phasor models. In other words, only the fundamental frequency component is represented in terms of magnitude and angle, disregarding the effects generated by harmonics in the device's semiconductor switching process.

The first conversion stage aims to perform the maximum power point tracking (MPPT). The MPPT algorithm used in this work is the Perturbation and Observation (P&O), which has as its operating principle the increase or decrease in the PV array voltage based on the increase or decrease in the generated power.

Converters are interconnected by a DC link, which is represented by an equivalent circuit of a capacitor connected in parallel to the inverter input, as shown in Fig. 2 and described by:

$$\frac{C}{2} \frac{d[V_{dc}^2(t)]}{dt} = P_g - P_t \quad (1)$$

The constant C is the DC link capacitance, P_g is the generated power by the PV array, and P_t is the power delivered to the network.

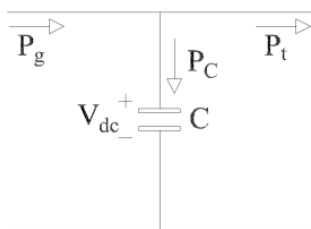


Fig. 2 DC link equivalent circuit.

In (1), it is seen that the DC link voltage being constant entails the equilibrium condition in which all the generated power is delivered to the grid.

DC-AC converter modeling is fundamental to understand the dynamics of the DC link, currents, and active and reactive power. The inverter is represented by a three-phase current controlled sources in the abc coordinates. The currents of these sources are obtained from Park transformations dq/abc from the direct axis (I_d^*) and quadrature axis (I_q^*) components in the synchronous reference frame in dq coordinates.

The expressions of the three-phase powers (P_t e Q_t) provided by the inverter to the grid are described by:

$$P_t = V_d I_d + V_q I_q \quad (2)$$

$$Q_t = V_q I_d - V_d I_q \quad (3)$$

where V_d is the direct axis voltage, V_q is the quadrature axis voltage, and I_d e I_q represent, respectively, the direct and quadrature axis current components.

Considering the direct axis of the dq frame aligned with the grid voltage, it follows that $V_q = 0$ and, therefore, active and reactive power can be controlled by acting on the inverter current components I_d and I_q , respectively.

Fig. 3 shows the DC-AC converter control structure with PI controller, the current limiter and the anti-windup represented. KP_1 and KP_2 are the proportional gains, Ti_1 and Ti_2 are the integral gains, and K_1 and K_2 are the anti-windup control gains.

The DC link voltage control loop (V_{dc}^*) acts on the d axis current component, which defines the active power delivered to the grid by the inverter, and the reactive power control loop (Q_t^*) acts on the q axis current component, regulating the reactive power exchanged with the grid by the inverter.

PI controllers are provided with anti-windup action to prevent integral windup when control loop variables are saturated due to the converters current limiting (Farias, 2019).

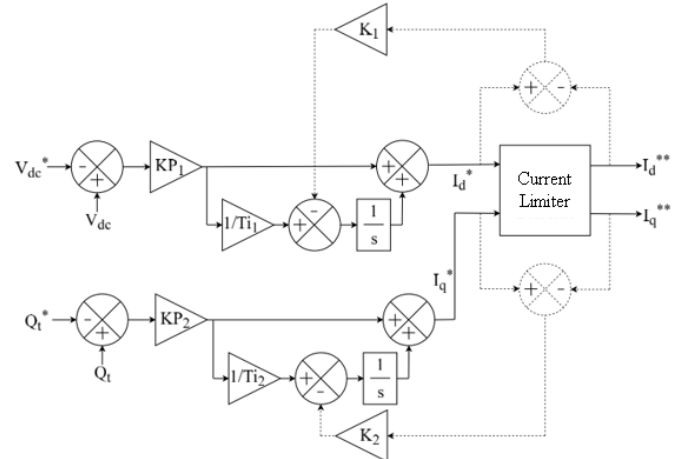


Fig. 3 DC-AC converter control structure.

Since the converter has limited current capacity, current references must be limited accordingly. The current references reaching the inverter are represented in dq coordinates, therefore, current limiting techniques are done on these components. In doing so, the performance of the Volt/Var control is affected, since the reactive power depends on the I_q component, as seen in (3).

In the case the current limiting seeks I_d priority, this component is limited to the maximum value of the total current, while I_q is limited to what remains of the inverter capacity, according to the equations:

$$I_{dsat} = \begin{cases} I_d, & \text{if } I_d \leq I_{max} \\ I_{max} & \text{if } I_d > I_{max} \end{cases} \quad (4)$$

$$I_{qmax} = \sqrt{(I_{max})^2 - (I_{dsat})^2} \quad (5)$$

In the case of I_q priority, I_q is limited to the maximum value of the total current and I_d is then limited to the remaining converter current capacity, as described by:

$$I_{qsat} = \begin{cases} I_q, & \text{if } I_q \leq I_{max} \\ I_{max} & \text{if } I_q > I_{max} \end{cases} \quad (6)$$

$$I_{dmax} = \sqrt{(I_{max})^2 - (I_{qsat})^2} \quad (7)$$

The modelled system will be used as a basis for the development of controls available in Smart Inverters, such as reactive power control to regulate local voltage, which will be presented next.

3. VOLTAGE CONTROL STRATEGIES

Recently, interconnection standards from different nations across the world requires renewable energy systems to have grid support controls due to the growing threat to voltage stability. For example, IEEE 1547-2018, in addition to providing the disconnection times during under-voltages and over-voltage events, also establishes controls to provide grid stability support (Naidu et al., 2019).

A. Smart Inverter Dynamic Voltage Support

Fig. 4 illustrates the Continuous Operation and Low Voltage Ride-Through (LVRT) Regions of the DG system, established in IEEE 1547-2018. Thus, during voltage sags, when grid voltage is between 0.65 p.u. and 0.88 p.u., DG operates within the region called LVRT, required to remain connected.

Furthermore, during the LVRT operation, the standard allows the DG to provide dynamic voltage support through the exchange of reactive and active power with the grid. In this paper, we wish to explore the Volt-VAr control for this purpose.

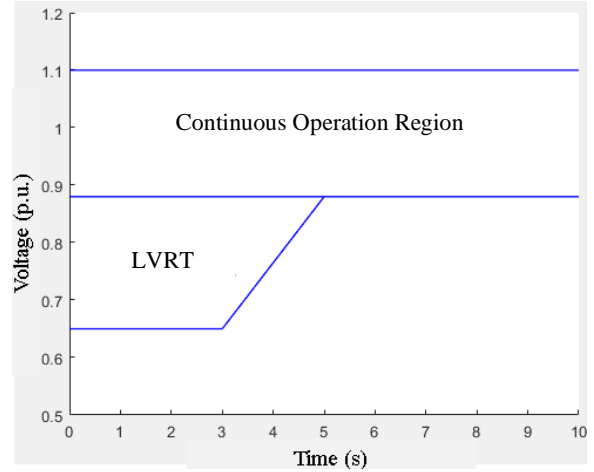


Fig. 4 Voltage Ride-Through requirements.

Volt-Var control can provide dynamics regulation response based on the local voltage of the power system. The inverter can either absorb or inject reactive power if the terminal voltage exceeds predefined upper or lower limits, respectively.

Fig. 5 is a Volt-Var control characteristic curve. For low voltage levels (lower than V_2), the inverter operates with capacitive power factor, injecting reactive power into to grid. Furthermore, for high voltage levels (higher than V_3), the inverter operates with inductive power factor, absorbing reactive power (Gonçalves, 2018).

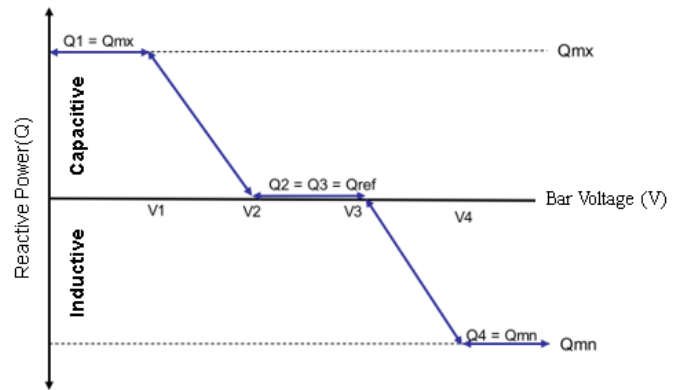


Fig. 5 Volt-VAr Control Curve.

In this work, the smart inverter is provided with Volt-Var control based on the characteristic curve shown in Fig. 5. The values of V_1 and V_2 used are 0.65 p.u. and 0.88 p.u., respectively. Therefore, the reactive power values are obtained according to the equation:

$$Q_t^* = \begin{cases} Q_{max} & V < 0.65 \text{ p.u.} \\ \frac{-Q_{max}}{0.23}(V - 0.88) & 0.65 \text{ p.u.} \leq V \leq 0.88 \text{ p.u.} \\ 0 & 0.88 \text{ p.u.} < V < 1.05 \text{ p.u.} \end{cases} \quad (8)$$

The Volt-Var control thus provides the reactive power reference to the reactive power control loop in the inverter control structure (Fig. 3), as shown in Fig. 6.

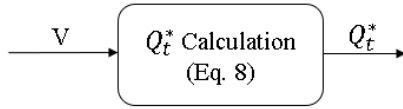


Fig. 6 Volt-Var Control structure.

Reactive power limits are calculated in accordance with the rated apparent power capacity of the inverter by:

$$|Q_{max}| = \sqrt{(S_{nom})^2 - P^2} \quad (9)$$

Thus, the maximum amount of reactive power that can be absorbed or injected into the grid at any instant considers the generated active power (P) at that moment and the rated power capacity (S_{nom}) of the Smart Inverter.

B. DC Link Control Strategies

The inverter ability to provide voltage support during faults is strongly connected to both the converter LVRT capacity and the converter current capacity. Strategies to deal with these aspects are developed in this section.

During faults, since the terminal voltage drops, the active current component tends to increase to keep the delivering of active power to the grid. Current capacity limits of the inverter may prevent the inverter to be able to deliver the whole PV generated power, causing the DC link voltage to increase, which may compromise the LVRT capacity of the inverter.

To address this issue, a control strategy that takes over the MPPT control algorithm during the fault period is proposed. The PV array is then forced to operate with a particular generated power P^* . The calculation of P^* is performed by three different strategies taken from Easley et al. (2020) and presented below.

These strategies change the maximum power point (MPP) through a reference power (P^*) according to the desired objective, which are:

Constant Peak Current: In this strategy, to maintain the injected peak current that occurred prior to the grid voltage sag, the harvested P_{fv} should reduce such that it is commensurate with the grid voltage sag and the active current component I_d . Thus, P^* is obtained from

$$P^* = |V| \times \sqrt{I_b^2 - I_q^2} \quad (10)$$

where I_b is taken as the inverter limit current capacity.

Constant Active Current: During voltage sags, the active current rises to maintain the power delivered to the grid. To avoid it, the harvest PV power should reduce such that it is commensurate with the grid voltage sag. Therefore, the power reference (P^*) is defined as:

$$P^* = PMPP \times V_{pU} \quad (11)$$

where V_{pU} is the terminal inverter voltage in p.u.

Constant Average Active Power: During faults and grid voltage sags, the reference power (P^*) is held constant at PMPP.

$$P^* = PMPP \quad (12)$$

Fig. 7 illustrates how the algorithm works. During normal operation, the Perturbation & Observation algorithm keeps the system operating at MPPT. During the fault period, identified by the voltage value being less than 0.9 p.u., the voltage support strategies take over, forcing the PV generated power to be regulated at P^* . For this study, K_C is set to 0,0002.

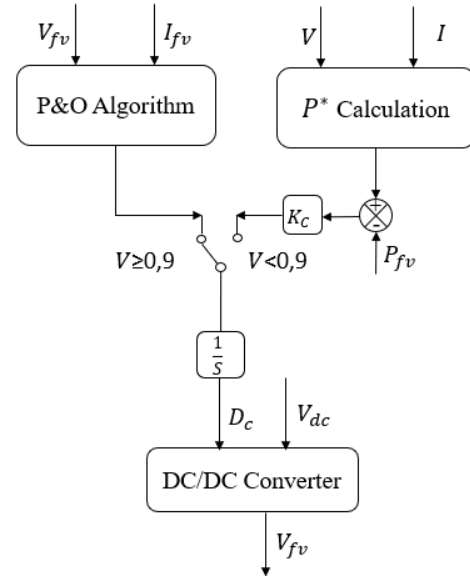


Fig. 7 DC Link Control Algorithm Operation.

Three different current prioritization techniques are considered for the converter current limitation. The first gives priority to the I_d component, or the delivering of active power. The second gives priority to I_q , leaving the whole inverter capacity available for reactive power exchange with the grid. The third strategy also gives priority to the I_q component, but up to the limit of 70% of the inverter capacity.

4. RESULTS

In this section, the developed DC link control strategies is applied to a PV smart inverter connected to a distribution system and simulations are provided illustrating its performance.

The whole system was modeled and simulated using MATLAB/Simulink. The PV array is composed by 250 solar panels that produce 200 W each; thus, the power harvested by the system is 50 kW.

The PV system is interconnected to a distribution network that supplies the Technological Center (CT) of the Federal University of Espírito Santo (UFES) campus and was adapted from a system taken from Silva's thesis (2014). Fig. 8 represents the UFES power system and the microgrid where DG is connected.

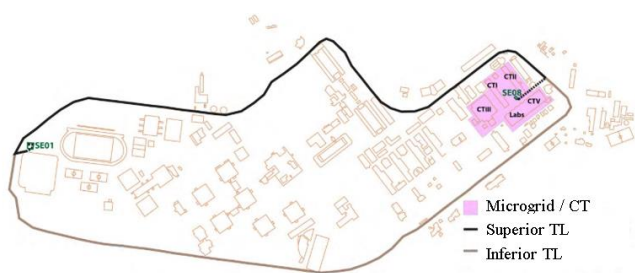


Fig. 8 UFES power system.

For this study, a three-phase fault is considered applied at the inverter terminals at 0.1 s, lasting 200 ms, with resistance of 1 Ω. The system operating point is at 1 p.u. (50 kW) of active power generated and unity power factor seen from the network. Fig. 9 illustrates the whole PV system that includes the PV array, the DC link, and the inverter, two loads (CTV and Lab. CT), the three-phase fault and the CT network.

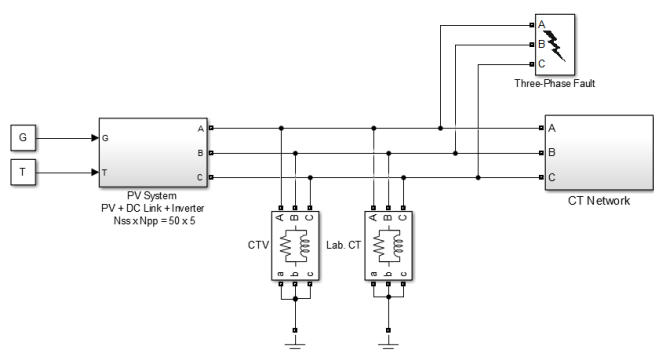


Fig. 9 Studied system with applied three-phase fault.

It will be evaluated how the Volt-VAr control performs as a dynamic voltage support during the fault period, considering the developed DC link voltage control strategies described in Section 3. The three cases will be considered for analysis and comparison:

Case 1: Constant Peak Current strategy;

Case 2: Constant Active Current strategy; and

Case 3: Constant Average Active Power strategy.

Each case is analyzed in conjunction with each of the three prioritization techniques: (i) I_d priority; (ii) I_q priority; (iii) weighed I_q priority, which uses 70% of the inverter capacity to supply reactive power.

Fig. 10 a), b), and c) describes the behavior of the generated reactive power for the three cases considering I_d , I_q and weighed I_q priority of the inverter current limiter, respectively.

It is seen that Case 1 uses I_q as a reference for calculating P^* , according to (10), leaving space for I_q and consequently reactive power injection. Thus, for all the current priorities, there is reactive power injection, as seen in Fig. 10 a), b) and c).

Case 2 keeps the active current component constant, that is why it is possible an increase in the I_q component through the Volt-VAr Control, and, consequently, reactive power injection. Thus, there is reactive power generation even considering I_d priority (Fig. 10 a) since the Case 2 leaves space for the Volt/VAr control operation.

In contrast, because of the I_d priority and the strategy principle to maintain the active power constant, there is no reactive power injection by the smart inverter in Case 3, as seen in Fig. 10 a). The inverter capacity is totally used to supply active power to the grid.

The reactive power is higher (reaching approximately 45 kVAr) when considering I_q priority than in the weighed I_q priority (reaching approximately 35 kVAr) because it uses 100% of the inverter capacity to supply reactive power.

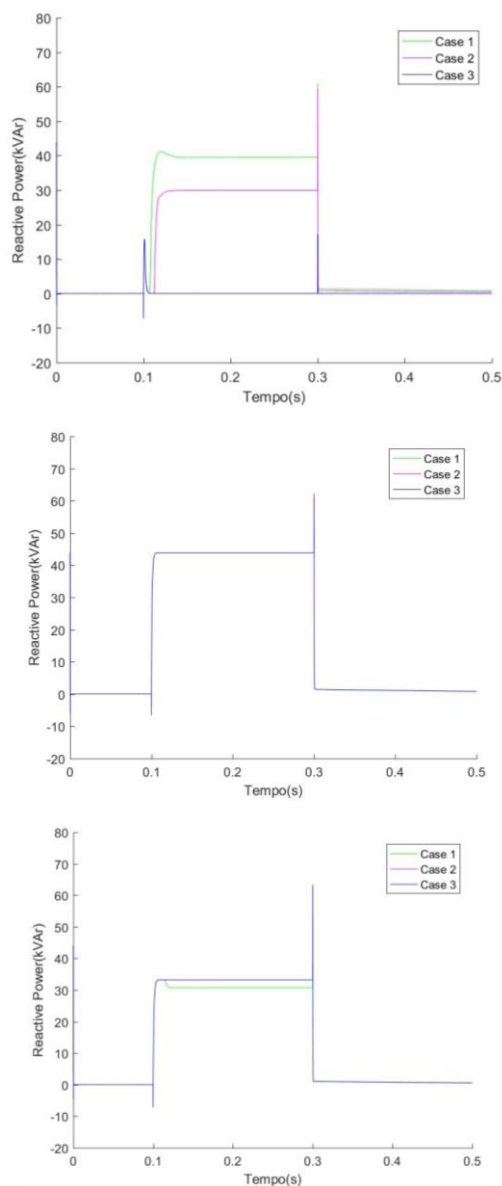


Fig. 10 Reactive power generated: a) I_d priority; b) I_q priority; c) bottom weighed I_q priority.

Fig. 11 a), b), and c) shows the behavior of the inverter terminal voltage for the three cases considering I_d , I_q and weighted I_q priority of the inverter current limiter, respectively. It is possible to observe that, during fault occurrence, the inverter terminal voltage drops below 300 V (0,79 p.u.).

But, with the maximization of the injected reactive power, considering I_q priority, the inverter terminal voltage was not better, as seen in Fig. 11 b). This is due to the resistive characteristic of the network, in which the active power has a greater influence on the voltage.

As a result, even using the inverter capacity to inject reactive power (priorities I_q and weighted I_q priority), the voltage does not necessarily show improvement, since it is also affected by the drop of the active power.

For example, Case 1 leaves more space to I_q , thus reactive power is higher in this case for all the current limiting. Consequently, the active power is lower, resulting in a worse terminal voltage, as seen in Fig. 11 a), b) and c).

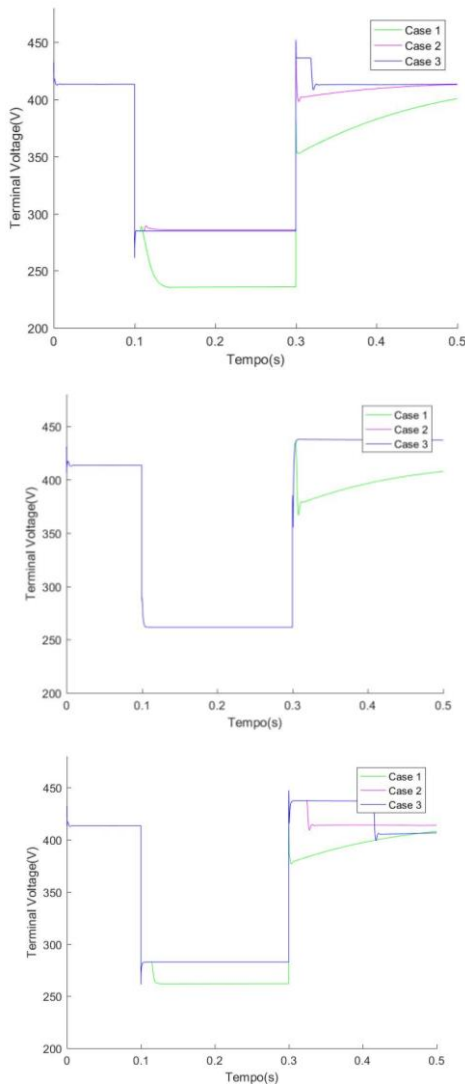


Fig. 11 Inverter terminal voltage: a) I_d priority; b) I_q priority; c) weighted I_q priority.

Fig. 12 a), b), and c) shows the behavior of the DC link voltage level for the three cases considering I_d , I_q and weighted I_q priority of the inverter current limiter, respectively.

As the goal of Case 3 is to maintain the active power generated by the PV array (P_{fv}) at the MPP, and the power injected to the system (P_t) drops according to the inverter terminal voltage during fault, the difference between P_{fv} and P_t causes an increase in V_{dc} , as shown in Fig. 12 a), b) and c).

Considering I_q and weighted I_q priority, this difference is even bigger for Case 3, because of the reactive power injection priority, which reduces P_t , resulting in a larger increase in V_{dc} , as shown in Fig. 12 b) and c).

In the other cases, V_{dc} tends to maintain, because these strategies try to achieve a balance between P_t and P_{fv} , reducing the harvest of P_{fv} . But, when considering I_q priority, there is almost no inverter capacity for active current I_d . Thus, even for Case 2 P_t is low, resulting in a larger increase in V_{dc} , as shown in Fig. 12 b).

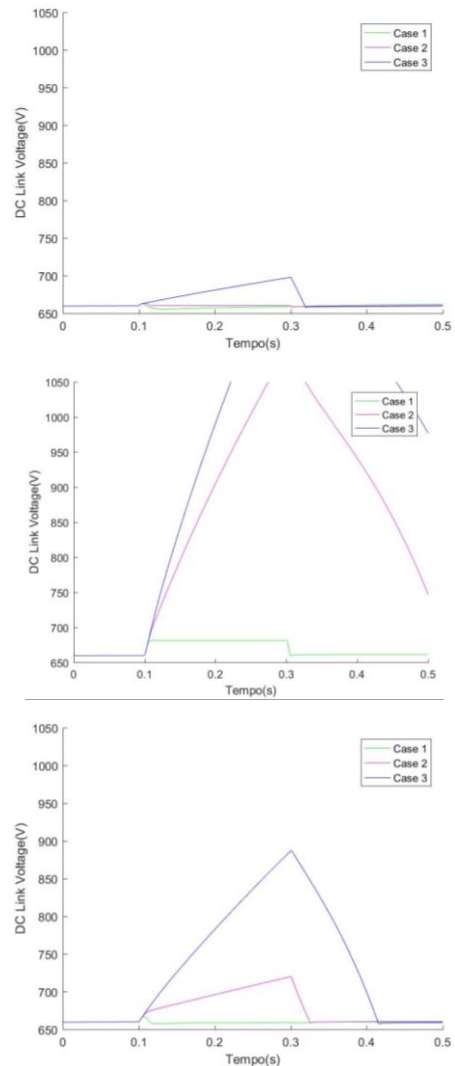


Fig. 12 DC link voltage level: a) I_d priority; b) I_q priority; c) weighted I_q priority.

5. CONCLUSION

This work explores the Volt-VAr control for dynamic voltage support during faults in smart inverters with LVRT capacity. Three different strategies to deal with DC link voltage level are also developed, because current capacity limits of the inverter may difficult the inverter to deliver the whole PV generated power, causing the DC link voltage to increase, and compromising the LVRT capacity. Strategies are analyzed considering three priority techniques for inverter current limiting.

In view of the graphs obtained, it was possible to use the inverter capacity for Volt-VAr control operation during the fault. However, there was no improvement in the voltage profile with the maximization of reactive power generation, due to the resistive characteristic of the network where the system is connected. Due to such characteristic, the active power has greater influence on the voltage.

Thus, weighted I_q priority was developed to weight the reactive and active power injection and try to improve the inverter terminal voltage. In conclusion, the best strategy observed was Case 2 with I_d priority, because the DC link voltage remained at lower levels, and the LVRT capacity of the inverter was not compromised. Furthermore, because this strategy keeps the active current component constant, the Volt-VAr control could operate, improving the inverter terminal voltage in conjunction with delivering active power.

REFERENCES

- Almeida, D., Pasupuleti, J., Ekanayake, J., & Karunarathne, E. (2020). Mitigation of Overvoltage Due to High Penetration of Solar Photovoltaics Using Smart Inverters Volt/Var Control. *Indonesian Journal of Electrical Engineering and Computer Science*, 19(3), 1259–1266. <https://doi.org/10.11591/ijeecs.v19.i3.pp1259-1266>
- ANEEL. (2019). O Brasil ultrapassa a marca de 1GW em geração distribuída. Available from: https://www.aneel.gov.br/sala-de-imprensa-exibicao/-/asset_publisher/XGPXSqdMFHrE/content/brasil-ultrapassa-marca-de-1gw-em-geracao-distribuida/656877. Accessed: march 2021.
- Arbab-Zavar, B., Palacios-Garcia, E., Vasquez, J., & Guerrero, J. (2019). Smart inverters for microgrid applications: A review. *Energies*, 12(5). <https://doi.org/10.3390/en12050840>
- Bravo, R.J. (2015). DER Volt-VAr and Voltage Ride-Through Needs to Contain the Spread of FIDVR Events. *IEEE Power and Energy Society General Meeting, 2015-Sept*, 1–3. <https://doi.org/10.1109/PESGM.2015.7286246>
- Easley, M., Jain, S., Shadmand, M., & Abu-Rub, H. (2020). Autonomous Model Predictive Controlled Smart Inverter with Proactive Grid Fault Ride-Through Capability. *IEEE Transactions on Energy Conversion*, 35(4), 1825–1836. <https://doi.org/10.1109/TEC.2020.2998501>
- Farias, G.A.B. (2019). Dinâmica durante faltas e controle de conversores aplicados a sistemas fotovoltaicos de geração distribuída interligados à rede elétrica. UNIOESTE.
- Gonçalves, B.C. (2018). Impactos do tipo de controle dos inversores da microgeração fotovoltaica na rede de distribuição. UFRJ.
- IEEE. (2018). Standard for Interconnection and Interoperability of Distributed Energy Resources with Associated Electric Power System Interface.
- Jafari, M., Olowu, T.O., & Sarwat, A.I. (2019). Optimal Smart Inverters Volt-VAR Curve Selection with a Multi-Objective Volt-VAR Optimization using Evolutionary Algorithm Approach. 2018 North American Power Symposium, NAPS 2018, 1–6. <https://doi.org/10.1109/NAPS.2018.8600542>
- Kashani, M.G., Mobarrez, M., & Bhattacharya, S. (2019). Smart Inverter Volt-Watt Control Design in High PV-Penetrated Distribution Systems. *IEEE Transactions on Industry Applications*, 55(2), 1147–1156. <https://doi.org/10.1109/TIA.2018.2878844>
- Lulbadda, K.T., & Hemapala, K.T.M.U. (2019). The additional functions of smart inverters. *AIMS Energy*, 7(6). <https://doi.org/10.3934/ENERGY.2019.6.971>
- Naidu, B.R., Bajpai, P., & Chakraborty, C. (2019). Voltage Fault Ride-Through Operation of Solar PV Units: A Review and Way Forward. 2019 8th International Conference on Power Systems: Transition towards Sustainable, Smart and Flexible Grids, ICPS 2019. <https://doi.org/10.1109/ICPS48983.2019.9067604>
- Shuvra, M.A., & Chowdhury, B.H. (2015). Integration of Solar Energy in Distribution System Through Smart Inverter Functionality. *2015 North American Power Symposium, NAPS 2015*, 1–6. <https://doi.org/10.1109/NAPS.2015.7335174>
- Silva, G.A.T. (2014). Modos de operação de uma microrrede de baixa tensão baseada em inversores de potência. UFES.
- Teodorescu, R., Liserre, M., & Rodríguez, P. (Electrical engineer). (2011). Grid converters for photovoltaic and wind power systems.
- Zhao, X., Chang, L., Shao, R., & Spence, K. (2018). Power System Support Functions Provided by Smart Inverters—A Review. *CPSS Transactions on Power Electronics and Applications*, 3(1), 25–35. <https://doi.org/10.24295/cpsstpea.2018.00003>